

# Anomalous elastic softening of $\text{SmRu}_4\text{P}_{12}$ under high pressure

Peijie Sun, Yoshiaki Nakanishi, Mitsuteru Nakamura, and Masahito Yoshizawa\*  
*Graduate School of Engineering, Iwate University, Morioka 020-8551, Japan*

Masashi Ohashi and Gendo Oomi  
*Department of Physics, Kyushu University, Fukuoka 810-8560, Japan*

Chihiro Sekine and Ichimin Shirotani  
*Faculty of Engineering, Muroran Institute of Technology, Muroran 050-8585, Japan*  
 (Dated: March 23, 2022)

The filled skutterudite compound  $\text{SmRu}_4\text{P}_{12}$  undergoes a complex evolution from a paramagnetic metal (phase I) to a probable multipolar ordering insulator (phase II) at  $T_{\text{MI}} \sim 16.5$  K, then to a magnetically ordered phase (phase III) at  $T_{\text{N}} \sim 14$  K. Elastic properties under hydrostatic pressures were investigated to study the nature of the ordering phases. We found that distinct elastic softening above  $T_{\text{MI}}$  is induced by pressure, giving evidence of quadrupole degeneracy of the ground state in the crystalline electric field. It also suggests that quadrupole moment may be one of the order parameters below  $T_{\text{MI}}$  under pressure. Strangely, the largest degree of softening is found in the transverse elastic constant  $C_T$  at around 0.5-0.6 GPa, presumably having relevancy to the competing and very different Grüneisen parameters  $\Omega$  of  $T_{\text{MI}}$  and  $T_{\text{N}}$ . Interplay between the two phase transitions is also verified by the rapid increase of  $T_{\text{MI}}$  under pressure with a considerably large  $\Omega$  of 9. Our results can be understood on the basis of the proposed octupole scenario for  $\text{SmRu}_4\text{P}_{12}$ .

PACS numbers: 62.20.Dc; 71.30.+h; 72.55.+s

## I. INTRODUCTION

$\text{SmRu}_4\text{P}_{12}$  is one of the more interesting members of the family of filled skutterudite  $\text{RT}_4\text{X}_{12}$  compounds ( $R$  = rare earths;  $T$  = Fe, Ru, Os;  $X$  = P, As, Sb) which shows a variety of physical properties including superconductivity, metal-insulator (MI) transition, magnetic ordering and heavy fermions (HF) [1, 2, 3]. The interest in  $\text{SmRu}_4\text{P}_{12}$  is due to its metal-insulator (MI) transition at  $T_{\text{MI}} \sim 16.5$  K, a subsequent antiferromagnetic (AFM) transition at  $T_{\text{N}} \sim 14$  K [3], and a strange  $H$ - $T$  magnetic phase diagram [4, 5].  $T_{\text{N}}$  is obscure at lower magnetic fields; however, it is distinctly visible in several measurements like thermal expansion [6] even in a zero magnetic field. With increasing magnetic field,  $T_{\text{MI}}$  increases while  $T_{\text{N}}$  decreases, resembling  $\text{CeB}_6$ , which has an antiferro-quadrupolar (AFQ) ordering and a subsequent magnetic ordering [7]. For this reason,  $\text{SmRu}_4\text{P}_{12}$  was initially thought to be an AFQ system; however, increasing doubt is being thrown on this view, stimulating interest in the order parameters (OPs).  $\text{SmRu}_4\text{P}_{12}$  crystallizes in a cubic structure with space group  $\text{Im}\bar{3}$  ( $T_h^5$ ), like other filled skutterudite compounds. Magnetic measurements show that Sm is trivalent with total angular momentum  $J = 5/2$ . Specific heat measurements suggest a crystalline electric field (CEF) scheme consisting of a  $\Gamma_{67}$  ground state quartet and an excited doublet  $\Gamma_5$  at about 60 K in the  $T_h$  symmetry [4, 8]. This scheme is plausible for understanding other measurements including the elastic

constant [9, 10]. Noticeably, the  $\Gamma_{67}$  quartet with both orbital and magnetic degeneracy, is a key point for understanding the various properties of  $\text{SmRu}_4\text{P}_{12}$ . Hydrostatic pressures of about 1 GPa in this work are assumed to have no substantial effects on the CEF scheme.

The AFQ scenario for  $\text{SmRu}_4\text{P}_{12}$  is under question as to several aspects. First, almost no elastic softening is observed above  $T_{\text{MI}}$  [9] and the elastic anomaly at  $T_{\text{MI}}$  is not very large, unlike a typical AFQ ordering such as in  $\text{CeB}_6$  [11] and  $\text{DyB}_2\text{C}_2$  [12]. Second, by application of magnetic fields, the specific heat anomaly of AFQ ordering in  $\text{CeB}_6$  is enhanced, while that at  $T_{\text{MI}}$  in  $\text{SmRu}_4\text{P}_{12}$  changes only slightly; meanwhile, the anomaly at  $T_{\text{N}}$  in  $\text{CeB}_6$  is weakened, whereas it is enhanced in  $\text{SmRu}_4\text{P}_{12}$  [7, 13]. Recently, the possibility of octupole ordering was proposed for the MI transition [14]. This proposition is based on the appearance of elastic softening in phase II toward  $T_{\text{N}}$  and the indistinctness of the subsequent magnetic ordering at  $T_{\text{N}}$ , because these facts suggest a new coupling of  $\Psi M \epsilon$  ( $\Psi$ : probable octupole OP in phase II;  $M$ : dipole OP in phase III;  $\epsilon$ : elastic strain induced by ultrasound) and indicate breakdown of the time reversal symmetry (TRS) in phase II. Breakdown of TRS is confirmed by muon spin relaxation ( $\mu\text{SR}$ ) [15], nuclear magnetic resonance (NMR) [16] and Sm nuclear resonant scattering [17] measurements. An AFQ ordering is non-magnetic and holds TRS, so is ruled out as the primary OP in phase II. On the other hand, an octupole ordering is magnetic and breaks TRS, so is possible in phase II. Microscopic measurements also suggest appearance of magnetic dipole moment in phase II even in a zero magnetic field, in addition to an unknown multipole ordering [16, 17]. This is very different to the strong candidate for

\*Electronic address: yoshizawa@iwate-u.ac.jp

octupole ordering material,  $\text{NpO}_2$  [18], which has only one phase transition.

An iso-structural compound,  $\text{PrRu}_4\text{P}_{12}$ , also shows MI transition ( $T_{\text{MI}} \simeq 63$  K) [19]. Its MI transition is accompanied by no magnetic anomaly, whereas a distinct magnetic anomaly is observed in  $\text{SmRu}_4\text{P}_{12}$ . Moreover, a structural distortion is observed in  $\text{PrRu}_4\text{P}_{12}$  [20] but is absent in  $\text{SmRu}_4\text{P}_{12}$ . These facts indicate a magnetic origin for the MI transition in  $\text{SmRu}_4\text{P}_{12}$ , unlike  $\text{PrRu}_4\text{P}_{12}$ . In fact, a charge density wave (CDW) due to Fermi surface nesting is plausible for interpreting the MI transition in  $\text{PrRu}_4\text{P}_{12}$  [21]. Recent X-ray and polarized neutron diffraction experiments have shown that the Pr-ion site splits into two nonequivalent crystallographic sites and suggest two different CEF schemes below  $T_{\text{MI}}$  [22], where the importance of the  $p$ - $f$  hybridization in the MI transition is also emphasized.

Ultrasonic measurement under hydrostatic pressures is rarely performed, partly due to its difficulty. We succeeded, however, in obtaining stable ultrasonic echoes by selecting a suitable sample of sufficient length. By performing such measurements, we intend to gain an insight into the following peculiarities in  $\text{SmRu}_4\text{P}_{12}$ . (1) The  $\Gamma_{67}$  quartet ground state degenerates with respect to  $\Gamma_3$  and  $\Gamma_5$ -type quadrupole moments; however, no distinct elastic softening is observed at ambient pressure. Application of hydrostatic pressures is expected to induce stronger quadrupole-strain and inter-site quadrupole interaction, which then affects elastic properties. Quadrupolar ordering, if visible under pressure, is helpful for understanding the possible OPs below  $T_{\text{MI}}$  and the peculiar  $H$ - $T$  phase diagram. (2) We intend to build a pressure-temperature ( $P$ - $T$ ) phase diagram from which to gain knowledge of the OPs of phase II and III. (3) One more point of interest is the very different Grüneisen parameters  $\Omega$  of  $T_{\text{MI}}$  and  $T_{\text{N}}$ , the latter being much larger than the former [23]. Widely different Grüneisen parameters suggest different pressure dependencies of the two phase transitions, and prompted us to explore the physical properties under hydrostatic pressures related to this phenomenon.

## II. EXPERIMENTS

A cylindrical polycrystalline  $\text{SmRu}_4\text{P}_{12}$  sample 4.1 mm in length and 3.4 mm in diameter was employed. It is the same one as used for ultrasonic measurements in magnetic fields [9] and was prepared at high temperatures and pressures using a wedge-type cubic anvil high-pressure apparatus. Actually, a single crystal is preferred here, but the available single crystals currently are very small, with dimensions of only  $1 \times 1 \times 1$  mm, preventing us from obtaining stable ultrasonic echoes under high pressures.

The relative change of sound velocity  $v$  was measured by means of a phase-comparison technique. This technique measures the relative  $\Delta v/v$  by detecting the relative frequency change  $\Delta f/f$  while keeping the phase shift at zero and neglecting any changes in sample length  $\Delta l/l$

(to be explained later). Elastic constant  $C$  is related to sound velocity  $v$  by the equation  $C = \rho v^2$ , where the density  $\rho$  of  $\text{SmRu}_4\text{P}_{12}$  is  $5.921 \text{ g}\cdot\text{cm}^{-3}$ .  $\text{LiNbO}_3$  piezoelectric plate with fundamental resonance frequency of 5-20 MHz was used as the ultrasonic transducer to both generate and detect the ultrasound. The only experimentally accessible ultrasound modes for a polycrystalline sample, i. e., longitudinal  $C_{\text{L}}$  propagating parallel to polarization and transverse  $C_{\text{T}}$  propagating perpendicular to polarization, were measured as a function of temperature under different hydrostatic pressures. The absolute values of  $C_{\text{L}}$ ,  $C_{\text{T}}$  and bulk modulus  $C_{\text{B}}$  of  $\text{SmRu}_4\text{P}_{12}$  at 100 K are 153, 24.6 and 120 GPa, respectively [9].

Hydrostatic pressure up to 1.15 GPa was generated using a Cu-Be piston-cylinder pressure cell and a Teflon capsule inside it. The cell has two layers, consisting of an outer cylinder and an inner one placed inside. The inner diameter and the length of the inner cylinder are 8 mm and 40 mm, respectively. The sample with two ultrasonic transducers bonded to it, together with a tin manometer, is placed in the Teflon capsule filled with pressure medium (a 1:1 mixture of Fluorinert FC 70 and FC 77). The measurements were carried out down to the temperature of liquid helium, 4.2 K, or down to  $\sim 1.5$  K by pumping. The effective hydrostatic pressure inside the Teflon capsule was calibrated by measuring the superconducting transition temperature of the tin manometer.

## III. EXPERIMENTAL RESULTS

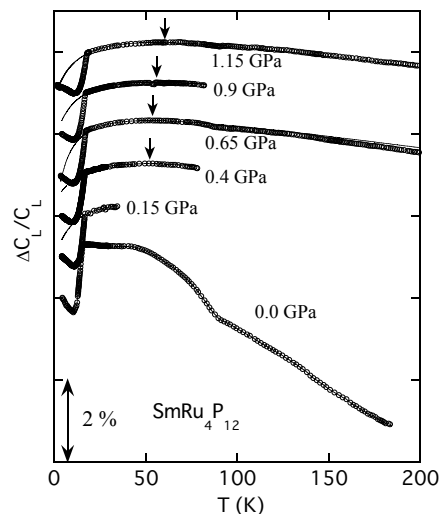


FIG. 1: Temperature dependence of the longitudinal elastic constant  $C_{\text{L}}$  under various pressures. The solid lines are calculated curves by Eq. (3). The arrows indicate  $T_{\text{soft}}$  below which elastic softening appears.

Fig. 1 shows the temperature dependence of the longitudinal mode  $\Delta C_{\text{L}}/C_{\text{L}}$  under various pressures. The solid lines are fitted curves that will be explained later.

The  $C_L$  at ambient pressure increases on cooling down to  $T_{MI}$  without elastic softening. Application of hydrostatic pressures induces a clear softening above  $T_{MI}$ , but its pressure dependence is very weak. This may be partially due to the relative hardness of  $C_L$  that includes bulk modulus  $C_B$ . The temperature  $T_{soft}$ , below which softening appears, shows a slight increase with increasing pressure.

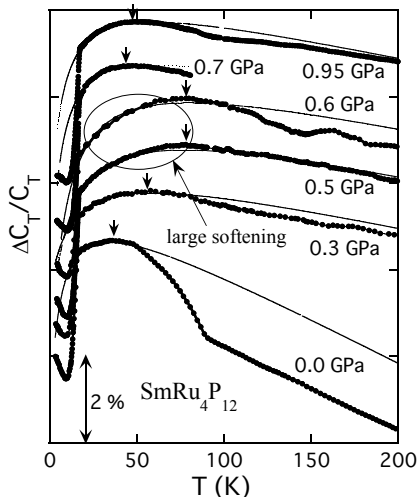


FIG. 2: Temperature dependence of the transverse elastic constant  $C_T$  under various pressures. The solid lines and arrows denote the same as in Fig. 1.

Fig. 2 shows the temperature dependence of the transverse mode  $\Delta C_T/C_T$  at various pressures, together with the fitted curves. Ambient pressure evidences a weak elastic softening above  $T_{MI}$  up to 35 K. With increasing pressure up to 0.6 GPa, elastic softening becomes increasingly marked. Furthermore,  $T_{soft}$  increases from 35 K for 0 GPa to about 80 K for 0.6 GPa. Strangely, upon further increasing the pressure by 0.7 GPa, the elastic softening fades again, while at the same time,  $T_{soft}$  also decreases. This strange pressure dependence presumably reflects the complexity of the phase diagram with two competing phase transitions. A kink structure is observed at around 90 K in both  $C_T$  and  $C_L$  at ambient pressure, reminiscent of the off-center motion of the  $R$  ions in the pnictogen cage, namely “rattling” as in  $\text{PrOs}_4\text{Sb}_{12}$  [24]. However, here it seems not due to an intrinsic origin because it is absent in single crystals. The kink becomes very weak or undetectable as soon as even a relatively weak pressure is applied; this is also not expected for a rattling motion.

For both  $C_L$  and  $C_T$ , a distinct slope change in the background  $C^0$ , is noticeable i.e., the lattice contribution to elastic constant, before and after applying pressure. As for the reasons, the influence of pressure-induced sample length variation  $\Delta l/l$ , which alters the relative ultrasound velocity as follows, is possible.

$$\frac{\Delta v}{v} = \frac{\Delta f}{f} - \frac{\Delta \varphi}{\varphi} + \frac{\Delta l}{l}. \quad (1)$$

Eq. (1) shows that in the phase-comparison technique, relative sound velocity  $\Delta v/v$  is composed of three parts, e.g., the relative frequency  $\Delta f/f$ , relative signal phase  $\Delta \varphi/\varphi$  and sample length  $\Delta l/l$ .  $\Delta \varphi/\varphi$  is kept at zero by a feedback loop that compares the phase shift between the ultrasonic signal transported by the sample and the reference signal.  $\Delta l/l$  is usually negligibly small. Therefore, this equation also explains why ultrasonic velocity  $v$  is measured as a shift in frequency. If  $\Delta l/l$  induced by pressure accounts for the change in  $C^0$ , the linear thermal expansion coefficient  $\alpha(T)$  is anticipated to be a change over  $5 \times 10^{-5} \text{ K}^{-1}$  under a pressure of about 0.3 GPa, in comparison with that at ambient pressure. This is at least an order of magnitude greater than the  $\alpha(T)$  at ambient pressure for  $\text{SmRu}_4\text{P}_{12}$  [6], making it impossible for  $\Delta l/l$  to account for the change in  $C^0$ . Although this peculiarity is not well understood, it does not affect our analysis of the elastic softening at low temperatures.

The temperature where a steep elastic drop occurs is known as the MI transition temperature  $T_{MI}$  at ambient pressure. Similarly, all such anomalies observed under pressure are ascribed to MI transition. Although significant elastic softening is induced by hydrostatic pressure, the shape of the abrupt anomaly at  $T_{MI}$  shows no substantial change. In fact, electrical resistance under high pressures remains characteristic of MI transition up to at least 1.2 GPa, while metallic behavior appears at  $P > 3.5 \text{ GPa}$  [25].  $T_{MI}$  increases on applying pressure, in agreement with the observations in electrical resistance. This issue will be discussed later in terms of Grüneisen parameter  $\Omega$ . Unfortunately, we can not detect an anomaly at  $T_N$  under pressure, as was successfully done in magnetic fields [9].

## IV. DISCUSSION

### A. Pressure-induced elastic softening

Symmetrized strains induced by ultrasound perturb CEF state via quadrupole-strain interaction  $g_\Gamma O_\Gamma \epsilon_\Gamma$ . Taking the inter-site quadrupole interaction  $g'_\Gamma O_\Gamma \langle O_\Gamma \rangle$  into account, elastic constant  $C_\Gamma$  can be formulated as follows by the second derivative of Landau free energy.

$$C_\Gamma(T) = C_\Gamma^0(T) - \frac{N g_\Gamma^2 \chi_\Gamma(T)}{1 - g'_\Gamma \chi_\Gamma(T)}. \quad (2)$$

Here  $C_\Gamma^0(T)$  is background elastic constant,  $N$  the number of  $R$  ions per unit volume,  $\chi_\Gamma(T)$  the corresponding strain susceptibility calculated using the CEF scheme, and  $g_\Gamma$  and  $g'_\Gamma$  are the coupling constants of the quadrupole-strain and quadrupole-quadrupole, respectively.  $C_\Gamma(T)$  measures the diagonal (Curie term) and non-diagonal (Van-Vleck term) quadrupolar matrix elements, analogous to the magnetic susceptibility that measures magnetic dipole matrix elements [26]. Analyzing the experimental results by using  $\chi_\Gamma(T)$ , one experimentally obtains  $|g_\Gamma|$  and  $g'_\Gamma$ .

At ambient pressure, no elastic softening was observed above  $T_{MI}$  for  $C_L$  and only very slight softening for  $C_T$ . Generally, this indicates a very weak quadrupole-strain coupling  $g_T$  for the  $\Gamma_{67}$  quartet ground state. This is believed to be a signature of complex multipolar ordering in phase II. On the other hand, a high degree of softening is observed under hydrostatic pressures, especially for  $C_T$ , giving evidence of the degeneracy of the CEF ground state with respect to quadrupole moment. Hydrostatic pressure induces elastic strain  $\epsilon_B = \epsilon_{xx} + \epsilon_{yy} + \epsilon_{zz}$  that corresponds to bulk modulus  $C_B$ .  $\epsilon_B$  has no direct couple with symmetry quadrupole moment  $O_\Gamma$ , thus is not a direct reason for the enhanced elastic softening.

A crucial point in the physics of the enhanced elastic softening is which of the two types of inherent quadrupole moments ( $\Gamma_3$  or  $\Gamma_5$ ) is responsible. The answer to this question may give direct insight into the OP symmetry of phase II; unfortunately, it can not be clarified based on the present results on a polycrystalline sample. In contrast to the symmetrized transverse modes in a single crystal like  $(C_{11} - C_{12})/2$  and  $C_{44}$  that respectively corresponds to  $\Gamma_3$  and  $\Gamma_5$ -type quadrupole moment,  $C_T$  and  $C_L$  in a polycrystalline sample reflect an average of different elastic modes. The former consists of  $C_{44}$  and  $(C_{11} - C_{12})/2$ ; the latter all the available modes including  $C_{11}$  and bulk modulus  $C_B$ . For the same reason, Eq. (2) cannot be directly used to analyze elastic softening here. Nevertheless, as long as the  $\chi_\Gamma(T)$  is dominated by the Curie term as predicted in the present system, Eq. (2) can be reformulated as follows.

$$C_\Gamma(T) = C_\Gamma^0(T) \left( \frac{T - T_C^0}{T - T_Q} \right). \quad (3)$$

According to Eq. (3), the quadrupole-strain coupling and inter-site quadrupole interaction can be evaluated as an average. Furthermore, transforming Eq. (3) to Eq. (4) is helpful in actual analysis.

$$\frac{1}{C_\Gamma^0(T) - C_\Gamma(T)} \approx \frac{T - T_Q}{T_C^0 - T_Q}. \quad (4)$$

Here  $T_Q = g_\Gamma^2 |\langle \varphi_i | O_\Gamma | \varphi_i \rangle|^2$  indicates the inter-site quadrupole interaction. The difference of the two characteristic temperatures,  $T_C^0 - T_Q = N g_\Gamma^2 |\langle \varphi_i | O_\Gamma | \varphi_i \rangle|^2 / C_\Gamma^0$ , is usually termed the Jahn-Teller coupling energy  $E_{JT}$  [27], and is a function of quadrupole-strain coupling.

Before analyzing elastic softening, elastic background  $C^0(T)$  should be carefully estimated. This process may affect the fitted values of  $T_Q$  and  $E_{JT}$  to some degree. Here we employ the commonly used  $T$ -linear  $C^0$ . Fig. 3 presents the measurement data of  $C_T$  and two estimated  $C^0(T)$  lines. All the curves at non-ambient pressures are superposed on each other and a common  $C^0(T)$  is estimated for them. Significantly, we found the pressure dependences of  $T_Q$  and  $E_{JT}$  to be almost independent of  $C^0(T)$  as long as a common background is employed as done in this Figure. In fact, a shared slope of all  $C_T(T)$  curves under non-ambient pressures at temperatures over

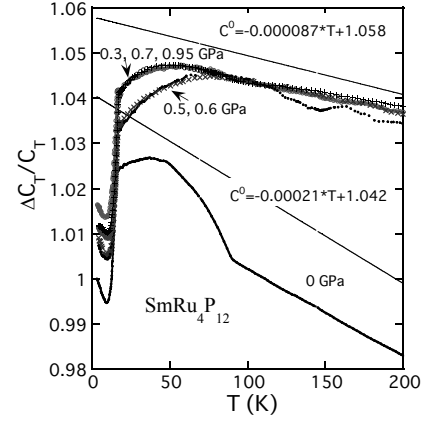


FIG. 3: Transverse elastic constant  $C_T(T)$  under various pressures that is superposed on each other. The two solid lines indicate estimated elastic background, described as  $C^0 = -0.00021 \times T + 1.042$  and  $C^0 = -0.000087 \times T + 1.058$ , for 0 GPa and other non-ambient pressures, respectively.

100 K can be observed, supporting the common  $C^0(T)$ . This procedure can maximally reduce extrinsic influence in estimating the two characteristic temperatures, and is crucial for the later discussions.

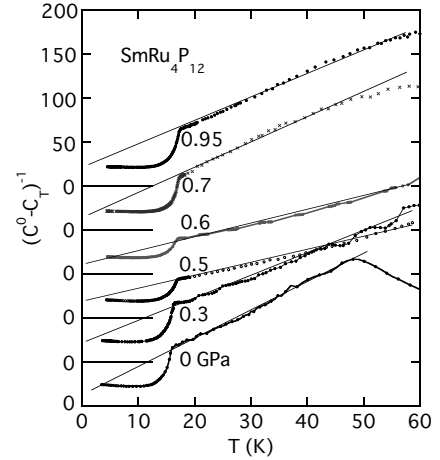


FIG. 4:  $(C^0 - C_T)^{-1}$  as a function of temperature under various pressures. The solid lines are Curie term fits based on Eq. (4), which give values of  $T_Q$  and  $E_{JT} = T_C^0 - T_Q$ .

Fig. 4 shows  $(C^0 - C_T)^{-1}$  as a function of temperature. The  $T$ -linear increase above  $T_{MI}$  conforms to the Curie term described by Eq. (4), due to the  $\Gamma_3$  and/or  $\Gamma_5$ -type quadrupole moment of the  $\Gamma_{67}$  ground state. The horizontal intercepts and the slopes of the linear fits give the quadrupolar interaction  $T_Q$  and Jahn-Teller coupling energy  $E_{JT}$ . For longitudinal  $C_L$  we performed the same procedure (not shown here). Note that the calculated curves shown in Fig. 1, 2 are based on the obtained  $T_Q$  and  $E_{JT}$  values, and Eq. (3).

Fig. 5 presents pressure dependence of the quadrupo-

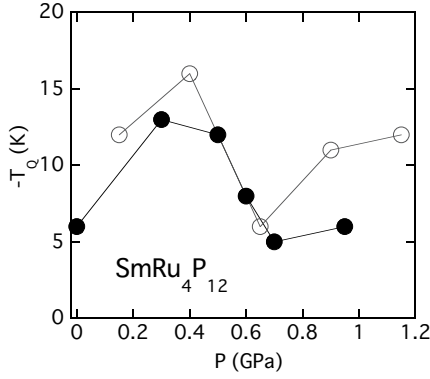


FIG. 5: Quadrupolar interaction  $T_Q$  as a function of pressure. Open circles denote data estimated from  $C_L$  and solid circles from  $C_T$ .

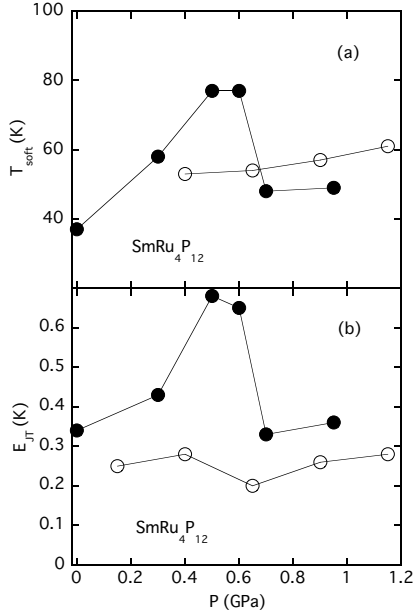


FIG. 6: Pressure dependences of (a) the temperature  $T_{\text{soft}}$  below which elastic softening appears, and (b) the Jahn-Teller energy  $E_{JT} = T_Q^0 - T_Q$ . Open circles denote data estimated from  $C_L$  and solid circles from  $C_T$ .

lar interaction,  $-T_Q$  vs.  $P$ .  $T_Q$ s are all negative in indication of antiferro-quadrupolar interaction.  $T_Q$  is once enhanced by pressure; however, it is weakened again at around 0.7 GPa where elastic softening is weakened. Shown in Fig. 6 are  $T_{\text{soft}}$  and Jahn-Teller energy  $E_{JT}$  as a function of pressure. Both of them depend on the same quadrupole-strain coupling and reflect the lattice instability. As expected,  $T_{\text{soft}}$  and  $E_{JT}$  show a similar pressure dependence. However, the two energies exhibit different pressure dependences for  $C_T$  and  $C_L$ ; enhanced values around 0.5-0.6 GPa are found in transverse  $C_T$ , while no distinct change is observed in longitudinal  $C_L$ .

Here we first discuss the pressure dependence of  $T_Q$  and  $E_{JT}$ . Because  $T_Q = g'_\Gamma |\langle \varphi_i | O_\Gamma | \varphi_i \rangle|^2$  and

$E_{JT} = N g_\Gamma^2 |\langle \varphi_i | O_\Gamma | \varphi_i \rangle|^2 / C_\Gamma^0$ , two possible explanations of their pressure dependences are available. (1) The two energies change with pressure due to changes in quadrupole moment  $|\langle \varphi_i | O_\Gamma | \varphi_i \rangle|$ . (2) Their changes are due to  $g'_\Gamma$  and  $g_\Gamma$ , respectively. For case (1), one expects a similar pressure dependence of  $T_Q$  and  $E_{JT}$ . This is different to our observations. Moreover, a significant change of the CEF scheme and the consequent quadrupole moment are not anticipated under the present hydrostatic pressures. The quadrupole Kondo effect may have an influence on  $|\langle \varphi_i | O_\Gamma | \varphi_i \rangle|$  but one would expect a screened quadrupole moment by applying pressure, not an enhanced one. Thus, it seems likely that changes in  $g'_\Gamma$  and  $g_\Gamma$  can be ascribed to the characteristic energies under pressure. Because  $g'_\Gamma \sim T_Q$  is negative and  $g_\Gamma^2 \sim E_{JT}$  is positive as factors in Eq. (2), the rapid decline of  $|T_Q|$  and enhancement of  $E_{JT}$  around 0.5-0.6 GPa will enhance elastic softening, consistent with the experimental facts in  $C_T$ . The absence of enhanced  $|T_Q|$  and  $E_{JT}$  in  $C_L$  within the present experimental accuracy remains an open question. Besides the hardness of  $C_L$ , which prevents a precise analysis of elastic softening, the difference between  $C_T$  and  $C_L$  may also suggest that the softening is due to one of the possible quadrupole modes,  $\Gamma_3$  or  $\Gamma_5$ , but not both.

## B. Increase of $T_{\text{MI}}$ with large Grüneisen parameter

Our results show that  $T_{\text{MI}}$  increases with pressure (Fig. 7), consistent with observations of electrical resistance [25]. It is also in agreement with thermal expansion measurements where lattice shrinkage is observed below  $T_{\text{MI}}$  [6]. The monotonic increase of  $T_{\text{MI}}$  with pressure contrasts strikingly with the unusual changes in  $T_Q$  and  $E_{JT}$ , suggesting again that the MI transition is not a quadrupolar ordering. Comparatively, no obvious pressure dependence [28] or a very slight increase [29] was observed for the  $T_{\text{AFQ}}$  in the typical AFQ compound  $\text{CeB}_6$ . Formula (5) defines the Grüneisen parameter as volume derivative of the phase transition temperature.

$$\Omega = -\frac{\ln T_{\text{MI}}}{\ln V} = \frac{C_B}{T_{\text{MI}}} \frac{\partial T_{\text{MI}}}{\partial P}. \quad (5)$$

Based on this formula, the Grüneisen parameter  $\Omega$  for  $T_{\text{MI}}$  is estimated to be 9 (solid line in Fig. 7). The pressure dependence of  $T_{\text{MI}}$  reported in ref. [25] leads to an  $\Omega$  of 7, roughly in agreement with ours. It is significant to make a comparison between the  $\Omega(T_{\text{MI}})$  of  $\text{SmRu}_4\text{P}_{12}$  and  $\text{PrRu}_4\text{P}_{12}$ . Performing the same calculation using the reported bulk modulus  $C_B = 207$  GPa [30] and the pressure dependence of  $T_{\text{MI}}$  [31], we obtain  $\Omega(T_{\text{MI}}) \simeq 2$  for  $\text{PrRu}_4\text{P}_{12}$ . The  $\Omega(T_{\text{MI}})$  for  $\text{PrRu}_4\text{P}_{12}$  is a normal value while that for  $\text{SmRu}_4\text{P}_{12}$  is large, again reflecting the essential difference between the two MI transitions.

The considerably large  $\Omega$  is reminiscent of the two very different Grüneisen parameters estimated for  $T_{\text{MI}}$  and  $T_N$  [23]. The conventional equation  $\Omega = C_B \beta / C$  (here  $\beta$  is

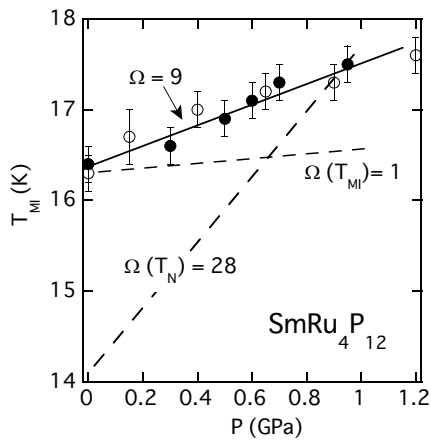


FIG. 7:  $T_{\text{MI}}$  as a function of pressure. The solid and open circles denote  $T_{\text{MI}}$  observed in  $C_{\text{T}}$  and  $C_{\text{L}}$ , respectively. The solid line is a guide for eyes and represents a Grüneisen parameter of  $\Omega = 9$ . The broken lines represent two supposed pressure dependences for  $T_{\text{N}}$  ( $\Omega = 28$ ) and  $T_{\text{MI}}$  ( $\Omega = 1$ ), respectively.

volume thermal expansion coefficient and  $C$  specific heat) gives a huge  $\Omega = 28$  for  $T_{\text{N}}$ , but a normal  $\Omega = 1$  for  $T_{\text{MI}}$ . Widely different  $\Omega$ s are expected to produce widely different pressure dependences of  $T_{\text{MI}}$  and  $T_{\text{N}}$ , as indicated by the broken lines in Fig. 7. Unfortunately, no magnetic fields were applied in this work, so  $T_{\text{MI}}$  and  $T_{\text{N}}$  are not separated and a more detailed  $P$ - $T$  phase diagram is not available. Noticeably, the  $\Omega = 9$  estimated in this work is smaller than that of  $T_{\text{N}}$  ( $\Omega = 28$ ) and larger than that of  $T_{\text{MI}}$  ( $\Omega = 1$ ). This is an evidence that the pressure dependence of  $T_{\text{MI}}$  derived from our measurements depends not only on the probable multipole OP in phase II but also on the magnetic OP in phase III. Instead, we think that separating  $T_{\text{N}}$  and  $T_{\text{MI}}$  under pressure is much more difficult than at ambient pressure due to the enhanced interplay between the two phases. In addition, the origin of the enormous  $\Omega(T_{\text{N}})$  may be approachable by HF behaviors. A large Grüneisen parameter is usually observed in HF systems [32] reflecting the large volume effect of the quasi  $p$ - $f$  hybridization band. Indeed, Kondo behaviors (e. g., the  $-\ln T$  dependence of electrical resistivity) are observed in  $\text{SmRu}_4\text{P}_{12}$  below 50 K [3] and elastic softening at low temperatures (below 3 K) similar to HF behavior is also observed [23].

A strong interplay between phases II and III suggested by the large  $\Omega$  hints at an octupole scenario for  $T_{\text{MI}}$  in  $\text{SmRu}_4\text{P}_{12}$ . This is clear because an octupole is magnetic, the same as the dipole OP in phase III, while the quadrupole is non-magnetic and holds TRS. In fact, a mix between OP of phase II (octupole) and OP of phase III (dipole) is proposed to explain the obscurity of the II-III phase transition in ref. [14]. Noticeably, enhanced elastic softening under pressure indicates that quadrupole moment may be one of the possible OPs in phase II or III under hydrostatic pressure. We infer two

possibilities for this enhanced elastic softening. First, quadrupole ordering is induced by pressures in phase II other than the primary OP, so  $|g_{\text{T}}|$  and thus elastic softening is enhanced by quadrupole fluctuation. Second, quadrupole moment is an accompanying or induced OP in phase III besides the magnetic dipole. Therefore, if  $T_{\text{N}}$  is really approaching  $T_{\text{MI}}$  as anticipated from the Grüneisen parameter analysis, the second inference will also produce enhanced elastic softening. There are three kinds of multipole ordering available in the  $\Gamma_{67}$  ground state [33], i. e., magnetic dipole, electric quadrupole, and magnetic octupole. Of these, octupole ordering may inherently induce quadrupole ordering ingredients, as in  $\text{NpO}_2$  [18], or may induce quadrupole ordering by the mode-mixing effect [14, 34], or by other mechanisms. Thus, induced quadrupole OP in phase II or III supports an octupole scenario for the MI transition. On the other hand, the largest elastic softening at around 0.5-0.6 GPa means a kind of criticality between the two transitions at this pressure, considering the very different Grüneisen parameters. In fact, the virtual temperature dependences of  $T_{\text{MI}}$  and  $T_{\text{N}}$  based on the Grüneisen parameters (broken lines in Fig. 7) cross at the same pressure. When increasing the pressure, the system presumably moves away from the criticality state and consequently the quadrupole-strain coupling and quadrupole fluctuation weakens again. This argument needs to be checked theoretically. Here it should be noted that we did not observe clear signs that  $T_{\text{N}}$  exceeds  $T_{\text{MI}}$  under pressure. So the trends of the two phase transition temperatures at pressures higher than the criticality remain an open question.

## V. SUMMARY

To summarize, we measured the longitudinal elastic constant  $C_{\text{L}}$  and transverse elastic constant  $C_{\text{T}}$  for polycrystalline  $\text{SmRu}_4\text{P}_{12}$  under hydrostatic pressure. Significant elastic softening is induced by hydrostatic pressure, especially in the transverse  $C_{\text{T}}$ . The results give evidence of degeneracy of the CEF ground state with respect to quadrupole moments. The enhanced elastic softening indicates that quadrupole moment may be one of the possible OPs in phase II or phase III under pressure. The MI transition is found to increase by applying pressure with a large Grüneisen parameter of 9. We also found that elastic softening above  $T_{\text{MI}}$  has a strange pressure dependence. The greatest elastic softening is observed at around  $P = 0.5$ - $0.6$  GPa, where the Jahn-Teller energy  $E_{\text{JT}}$  shows the largest values and  $|T_{\text{Q}}|$  decreases. This strangeness may be related to the enormous Grüneisen parameter of  $T_{\text{N}}$  in contrast to that of  $T_{\text{MI}}$ , and suggests a strong interplay between phase II and III. Our results prefer the octupole moment as the primary OP in phase II. Experiments in magnetic fields in addition to hydrostatic pressures are currently in progress, in order to separate the two successive transitions and establish a

detailed  $P$ - $H$ - $T$  phase diagram.

### Acknowledgments

This work is supported by Grant-in-Aid for Scientific Research Priority Area, Skutterudite (no. 15072202) of

the Ministry of Education, Culture, Sports, Science and Technology of Japan.

- 
- [1] E. D. Bauer, N. A. Frederick, P. -C. Ho, V. S. Zapf, and M. B. Maple, *Phys. Rev. B* **65** (2002) 100506(R).
  - [2] S. Sanada, Y. Aoki, H. Aoki, A. Tsuchiya, D. Kikuchi, H. Sugawara, and H. Sato, *J. Phys. Soc. Jpn.* **74** (2005) 246.
  - [3] C. Sekine, T. Uchiumi, I. Shirotni, and T. Yagi, in *Science and Technology of High Pressure*, ed. M. H. Manghnani, W. J. Nellis, and M. F. Nicol (Universities Press, Hyderabad, India, 2000) p. 826.
  - [4] K. Matsuhira, Y. Hinatsu, C. Sekine, T. Togashi, H. Maki, I. Shirotni, H. Kitazawa, T. Takamasu, and G. Kido, *J. Phys. Soc. Jpn.* **71** (2002) Suppl. 237.
  - [5] C. Sekine, I. Shirotni, K. Matsuhira, P. Haen, D. De Brion, G. Chouteau, H. Suzuki, and H. Kitazawa, *Acta Physica Polonica B* **34** (2003) 983.
  - [6] C. Sekine, Y. Shimaya, I. Shirotni, and P. Haen, *J. Phys. Soc. Jpn.* **74** (2005) 3395.
  - [7] J. M. Effantin, J. Rossat-Mignod, P. Burlet, H. Bartholin, S. Kunii, and T. Kasuya, *J. Magn. Magn. Mater.* **47&48** (1985) 145.
  - [8] K. Takegahara, H. Harima, and A. Yanase, *J. Phys. Soc. Jpn.* **70** (2001) 1190.
  - [9] M. Yoshizawa, Y. Nakanishi, T. Kumagai, M. Oikawa, C. Sekine, and I. Shirotni, *J. Phys. Soc. Jpn.* **73** (2004) 315.
  - [10] M. Yoshizawa, Y. Nakanishi, T. Kumagai, M. Oikawa, S. R. Saha, H. Sugawara, and H. Sato, *Physica B* **359-361** (2005) 862.
  - [11] S. Nakamura, T. Goto, S. Kunii, K. Iwashita, and A. Tamaki, *J. Phys. Soc. Jpn.* **63** (1994) 623.
  - [12] Y. Nemoto, T. Yanagisawa, K. Hyodo, T. Goto, S. Miyata, R. Watanuki, and K. Suzuki, *Physica B* **329-333** (2003) 641.
  - [13] K. Matsuhira, Y. Doi, M. Wakeshima, Y. Hinatsu, H. Amitsuka, Y. Shimaya, R. Giri, C. Sekine, and I. Shirotni, *J. Phys. Soc. Jpn.* **74** (2005) 1030.
  - [14] M. Yoshizawa, Y. Nakanishi, M. Oikawa, C. Sekine, I. Shirotni, S. R. Saha, H. Sugawara, and H. Sato, *J. Phys. Soc. Jpn.* **74** (2005) 2141.
  - [15] K. Hachitani, H. Fukazawa, Y. Kohori, I. Watanabe, C. Sekine, and I. Shirotni, *Phys. Rev. B* **73** (2006) 052408.
  - [16] S. Masaki, T. Mito, N. Oki, S. Wada, and N. Takeda, *J. Phys. Soc. Jpn.* **75** (2006) 053708.
  - [17] S. Tsutsui, Y. Kobayashi, T. Okada, H. Haba, H. Onodera, Y. Yoda, M. Mizumaki, H. Tanida, T. Uruga, C. Sekine, I. Shirotni, D. Kikuchi, H. Sugawara, and H. Sato, *J. Phys. Soc. Jpn.* **75** (2006) 093703.
  - [18] J. A. Paixão, C. Detlefs, M. J. Longfield, R. Caciuffo, P. Santini, N. Bernhoeft, J. Rebizant, and G. H. Lander, *Phys. Rev. Lett.*, **89** (2002) 187202.
  - [19] C. Sekine, T. Uchiumi, I. Shirotni, and T. Yagi, *Phys. Rev. Lett.* **79** (1997) 3218.
  - [20] C. H. Lee, H. Matsuhara, A. Yamamoto, T. Ohta, H. Takazawa, K. Ueno, C. Sekine, I. Shirotni, and T. Hirayama, *J. Phys.: Condens. Matter* **13** (2001) L45.
  - [21] H. Harima and K. Takegahara, *Physica B* **312-313** (2002) 843.
  - [22] K. Iwasa, L. Hao, T. Hasegawa, T. Takagi, K. Horiuchi, Y. Mori, Y. Murakami, K. Kuwahara, M. Kohgi, H. Sugawara, S. R. Saha, Y. Aoki, and H. Sato, *J. Phys. Soc. Jpn.* **74** (2005) 1930.
  - [23] M. Yoshizawa, Y. Nakanishi, T. Tanizawa, A. Sugihara, M. Oikawa, P. Sun, H. Sugawara, S. R. Saha, D. Kikuchi, and H. Sato, *Physica B* **378-380** (2006) 222.
  - [24] T. Goto, Y. Nemoto, K. Sakai, T. Yamaguchi, M. Akatsu, T. Yanagisawa, H. Hazama, K. Onuki, H. Sugawara, and H. Sato, *Phys. Rev. B* **69** (2004) 180511(R).
  - [25] A. Miyake, I. Ando, T. Kagayama, K. Shimizu, C. Sekine, K. Kihou, and I. Shirotni, *J. Alloy and Compound* **408-412** (2006) 238.
  - [26] P. Thalmeier and B. Lüthi, in *Handbook on the Physics and Chemistry of Rare Earths*, edited by K. A. Gschneidner *et al.* (North-Holland, Amsterdam, 1991), Vol.14.
  - [27] K. I. Kugel and D. I. Khomskii, *Usp. Fiz. Nauk* **136** (1982) 621 [*Sov. Phys. Usp.* **25** (1982) 231].
  - [28] S. Sullow, V. Trappe, A. Eichler, and K. Winzer, *J. Phys.: Condens. Matter* **6** (1994) 10121.
  - [29] Y. Uwatoko, K. Kosaka, M. Sera, and S. Kunii, *Physica B* **281&282** (2000) 555.
  - [30] I. Shirotni, J. Hayashi, T. Adachi, C. Sekine, T. Kawakami, T. Nakanishi, H. Takahashi, J. Tang, A. Matsushita, and T. Matsumoto, *Physica B* **322** (2002) 408.
  - [31] A. Miyake, T. Kagayama, K. Shimizu, C. Sekine, K. Kihou, and I. Shirotni, *Physica B* **359-361** (2005) 853.
  - [32] B. Lüthi and M. Yoshizawa, *J. Magn. Magn. Mater.* **63&64** (1987) 274.
  - [33] R. Shiina, H. Shiba, and P. Thalmeier, *J. Phys. Soc. Jpn.* **66** (1997) 1741.
  - [34] Y. Kuramoto and H. Kusunose, *J. Phys. Soc. Jpn.* **69** (2000) 671.